Al-Rafidain Journal of Computer Sciences and Mathematics (RJCSM)

www.csmj.uomosul.edu.iq

An Advanced GAN-Based Framework for Medical Image Enhancement

Saja Younis Hamid Alhamdani

Department of Artificial Intelligence, College of Computer Science and Mathematics, University of Mosul, Iraq
Email: sata@uomosul.edu.iq

Article information

Article history:
Received 1 June, 2025
Revised 25 July, 2025
Accepted 17 August, 2025
Published 25 December, 2025

Keywords:
Image Enhancement,
Medical image,
GAN algorithm.

Correspondence:
Saja Younis Hamid Alhamdani
Email: sata@uomosul.edu.iq

Abstract

Low contrast, noise, and low visual detail are major medical image problems that pose a negative effect on diagnostic accuracy. This paper suggests a more developed model using deep generative networks (GANs) to enhance the quality of medical iris images. The framework has a sequence of preprocessing steps that include contrast enhancement (CLAHE), noise removal (Bilateral Filter), and edge enhancement (Unsharp Masking), and then the stage of enhanced generation with an attention-assisted generator (Adam) with fine-tuned parameters. SSIM, PSNR and LPIPS measures were used to evaluate the performance of the model. The findings revealed that there were significant visual and perceptual structure of images as results showed that, average SSIM was improved by 0.9383 to 0.9783, LPIPS was reduced by 0.0137 to 0.0078 and PSNR had increased by 28.62 to 32.23 than the default parameters. These results confirm the usefulness of fine-tuning at enhancing perceptual and structural image measures. This model improves the diagnosis abilities in the medical field and minimizes the use of costly refined imaging methods, hence it can be applied in large scale clinical setting.

DOI: 10.33899/rjcsm.v19i2.60304,

1. Introduction

Healthcare professionals heavily rely on medical imaging for diagnosis and treatment planning in various medical fields, and an adequate amount of image data from multiple and diverse devices contributes to patient safety and diagnostic accuracy [1]. Medical image acquisition devices use imaging sensors to transform non-visible texture features, such as density, contrast, and reflection, into digital intensity values, recorded to create a diagnostic image [2].

The advancement of imaging technologies has opened new horizons in visualizing the human body in bizarre ways. Nowadays, imaging plays an indispensable role across all fields of healthcare, including nuclear imaging, computed tomography, magnetic resonance imaging, and more. All of these different types of imaging techniques produce different modalities of images and must be viewed and reconstructed in a proper way for optimal results. [3]. Better and more accurate software is a key component of a comprehensive data analysis and assessment tool.

Due to the unavailability of image enhancement technologies in the medical field, diagnostic images often suffer from reduced brightness, contrast, and clarity, which impairs the quality of medical imaging and makes diagnosis difficult, especially in complex medical cases. [4] [5].

Image enhancement is a procedure of improving the quality of an image; sometimes, this refers to restoration or reconstruction [6]. Enhancement consists of both image sharpening (via a Laplace filter) and image smoothing (using a Gaussian blur filter) to enhance contrast while preserving edge details and minimizing noise [7]. Image smoothing generally is an operation that reduces the prominence of the variation of tone concerning the local average [8]. Most smoothing operations act to suppress high frequencies, which correspond to detail, so the operation is sometimes referred to as low-pass filtering. In image processing, an image may be degraded or corrupted, or too much noise may be added. Many existing restoration techniques fail to give satisfactory results in the presence of noise [9]. Simple schemes such as averaging filters, Wiener filters, or Kalman

filters can be very effective when designed to work with low, wide-band Gaussian noise. However, they all fail in the presence of heavy noise and other non-Gaussian noise distributions [10].

Image enhancement algorithms are a crucial tool in enhancing the efficiency and accuracy of medical image analysis. They improve image characteristics, making it easier for physicians to detect pathological details, increasing the reliability of clinical assessment and decision-making effectiveness [11]. The enhancement algorithms for digital images have been studied earlier to improve their quality. However, most of the methods are based on classical approaches such as histogram equalization, contrast stretching, etc. [12]. They usually focus on enhancing their contrast and brightness.

Recently, with the blooming of artificial intelligence research interests, as skill gaps have been reduced between humans and computers [13], It has been observed that there has been a rapid development of image enhancement algorithms based on neural networks. Currently, deep neural networks have been widely used in numerous applications ranging from natural image processing to all optical, acoustic, and radar-systems related inverse-scatterings and reconstructions [14]. Among the neural network architectures, Generative Adversarial Networks (GANs) have shown exceptional promise in medical image enhancement tasks. GANs consist of two competing networks—a generator and a discriminator—that learn through adversarial training to produce high-fidelity images [5]. Despite their success, many existing models rely on default training parameters.

Based on the above challenges in medical image quality and visual detail accuracy, this research aims to develop an advanced framework based on deep generative networks (GANs) to enhance medical iris images in terms of contrast, noise reduction, and fine detail enhancement. A series of preprocessing steps is adopted, followed by an improved generation model that incorporates spectral normalization in the discriminator to address instability during training our model, which helps control gradient magnitudes and stabilizes the adversarial learning process. This is supported by the Adam initialization algorithm and hyperparameters, to achieve a balance between visual accuracy and computational efficiency. This study addresses this gap by evaluating the effect of hyperparameter optimization on the quality of GAN-generated medical images. It focuses on demonstrating the effectiveness of the proposed model through quantitative evaluation using SSIM, PSNR, and LPIPS metrics, which reflect the level of improvement in the quality of the resulting images.

2. Related Work

In recent years, deep generative networks (GANs) have emerged as a promising tool in medical image enhancement, due to their effective contribution to restoring fine visual details and enhancing the quality of images that suffer from low resolution or noise, which are often caused by limitations in imaging equipment or reduced radiation dose. Among the notable works: In a study by Mahboubisarighieh et al. [15], Researchers developed a GAN-based model to improve the quality of medical radiographic images. The model was based on a perceptual learning algorithm and was applied to dental radiographs, where it demonstrated a significant improvement in image quality. The evaluation results were: SSIM ≈ 0.848, PSNR ≈ 25.46 dB, and LPIPS = 0.152. These results reflect the effectiveness of the model compared to traditional methods, but they are still below optimal levels for high-quality diagnostic images. Abdusalomov et al. [16] presented a proposal based on the SRGAN model to enhance medical images in low-light conditions, focusing on restoring fine details and improving image quality. The study evaluated the model's performance using objective metrics, including PSNR and SSIM, with values of 28.45 dB and 0.8423, respectively. These results indicate acceptable effectiveness of the model, but they still fall short of the ideal performance required for high-resolution medical images.

3. Technical Background

3.1. Image Preprocessing Techniques

Noises often distort images. Noise is an unwanted disturbance that generally occurs while capturing photos or when the image is transmitted from one channel to another. [17]. The atmosphere of the image affects it due to various reasons, such as blurriness, pixelization, brightness, etc. To eliminate this noise, add some distortion to itself, which is generally termed as noise, and the removal of this noise is a crucial task, and it depends on the noisy image; with this original image, it can be regenerated [18].

Image Denoising. Depending on the application, an image filter may need to enhance features of interest and/or reduce those that contain noise. Such applications are particularly useful in medical imaging, remote sensing, photographic display, and archiving [19]. Several filtering techniques have been proposed for this purpose. These schemes may be categorized as either linear or nonlinear procedures. Linearity refers to operations in which the output pixel, such as an arithmetic mean, can be computed directly as a linear view of a subset of pixel values centered about the target pixel. With linear filters, such as Gaussian filters, the gray values of filtered images are a linear combination of the original quantities. The constraints of linearity are such that the output of an input function is a function only of a linear combination of its components. Nonlinear methods represent pixel values in terms of a nonlinear function [20] [21].

3.2. CLAHE

Contrast is an essential feature of an image. An image will appear more natural, more stunning, and transmit more detail and information if the contrast in the photo is more reasonable

or optimal. Contrast enhancement for enhancing the visual appearance of a distorted image is one of the leading research problems in digital image processing [22]. A widely adopted example is contrasting limited adaptive histogram equalization (CLAHE), which performs local adjustments in image contrast with low noise amplification [23]. These contrast adjustments are interpolated between patches of neighboring images called kernels. CLAHE achieves spatial adaptivity through the selection of kernel size. The intensity range of the kernel histogram, set by a clip limit, restrains noise amplification [24] [25].

3.3. Bilateral filtering noise reduction

A bilateral filter is a nonlinear filtering technique for image processing. It is a noniterative and edge-preserving filter that replaces the value of a pixel, which is only what it makes of itself and the surrounding pixels, with a weighted average of its spatial neighbors [6] [26]. It has been used in image denoising to eliminate noise while preserving edges in photographs, and in computer graphics to maintain sharpness in 2D and 3D images [27] [28].

3.4. Sharpening via unsharp masking

The unsharp masking technique is a popular image processing technique for enhancing sharpness in photographic images [29]. The method employs a technique in which an enhanced frame is obtained by superimposing a blurred image and an enhanced image that are derived from a reference image [30]. Mathematical models of the information loss in a Gaussian blurring process, as well as the ringing artifacts produced in the unsharp masking method, have been formulated [31].

3.5. Generative Adversarial Networks (GANs)

Generative Adversarial Networks (GANs) are now very famous in the machine learning community and are a very popular model for image generation tasks. In its early stage, GANs were adapted to the medical imaging area to generate medical images for a moderately sized dataset [32]. The key idea of GANs is to train a generator and a discriminator; the generator creates fake images to confuse the discriminator. In contrast, the discriminator attempts to tell apart which images have real labels and which ones are fake. The two networks confront each other, and their performances improve with each iteration. Eventually, when the generator is sufficiently improved, it can generate realistic images that are indistinguishable from real ones [33], As in Figure 1. GANs are appropriate for cases when insufficient real data is a problem, as they generate additional fake data. Besides, GANs have an advantage over other image synthesis approaches since GANs explicitly learn distributions of the underlying training sample data rather than explicitly modeling the image signal formation process [34] [35].

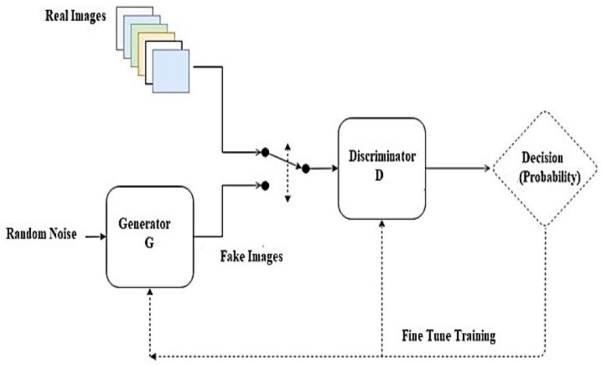

Figure 1. Schematic Block Diagram of Generative Adversarial Network (GAN) [33].

3.6. Evaluation Metrics

To maintain and control the quality of an image using image compression systems or to enhance the quality of the image using image enhancement systems, it is essential to assess the image's quality. Since quality assessment is directly related to the ability of the observer to discriminate between signal and noise, an accurate quality assessment is generally required to be subjectively measured. [36]. The Human Visual System (HVS) is the final recipient of any visual information, and its knowledge plays a vital role in constructing accurate models for measuring image quality.

Structural Similarity Index Measure (SSIM): Structural Similarity Index (SSIM) is a perceptually motivated measure of the quality of a visual signal, where the range is between -1 and 1, and it is equal to 1 if the two images are the same [37]. The mathematical formulation for the standard implementation mode of SSIM is given together with theoretical proofs of the definition of the quality index and the constants used to prevent divisions by zero [38].

Learned Perceptual Image Patch Similarity (LPIPS): There are several thorough investigations into the flaws of existing deep perceptual similarity metrics and the properties of human perception [39]. The perceptual similarity of image patches is tightly linked to their semantic similarity [40]. Dimensions perceptually judged by humans can be challenging to learn from simple data reduction techniques. (LPIPS) It is a neural-network-based perceptual metric that compares deep feature activations across image patches. It correlates more closely with human judgments of similarity compared to traditional pixel-level metrics [41].

Peak Signal-to-Noise Ratio (PSNR): Peak Signal-to-Noise Ratio (PSNR) is a widely used metric in image processing, particularly for assessing image coding algorithms. PSNR is a widely used metric to measure the quality of reconstructed images by comparing the peak signal value of the ground truth image with the super-resolution algorithm's error. PSNR is

commonly used to assess the performance of SR algorithms due to its computational efficiency and ease of implementation [42].

4. Methodology

Our methodology, as shown in Figure 1, it illustrates the sequential stages of the proposed system, starting from the initial setup to the final evaluation and saving of results. The pre-processing phase incorporates three enhancement techniques — Contrast Limited Adaptive Histogram Equalization (CLAHE), Bilateral Filtering, and Unsharp Masking — to improve image clarity before passing the data to the Model and training phase and then to the evaluation and saving phase.

4.1. Pre-processing phase: began with a comprehensive preprocessing phase aimed at preparing the medical iris images for deep learning enhancement. Each image was first converted to grayscale and resized to ensure compatibility with convolutional architectures. To improve local contrast while preserving fine details, we applied adaptive CLAHE. Noise reduction was handled using a brilliant bilateral filtering technique, which effectively removed noise without sacrificing important structural features. To further highlight critical details, a sharpening filter was applied, resulting in more transparent and more diagnostic images.

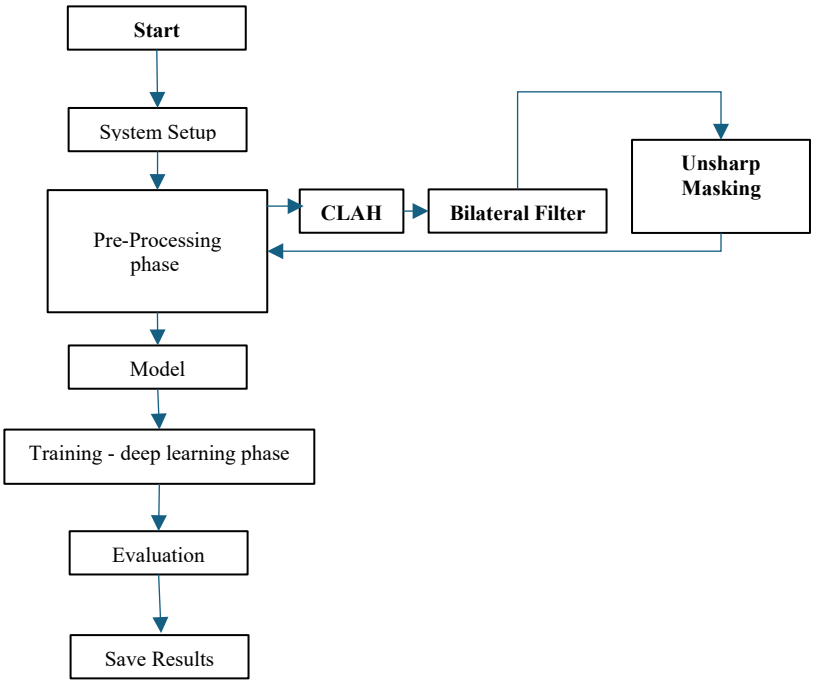

Figure 2. Flowchart of the proposed medical image enhancement framework.

4.2. Model and training phase: In this phase, the pre-processed medical images are fed into a custom-designed deep learning model built upon a generative architecture integrated with spectral normalization to stabilize the training of the discriminator and prevent exploding gradients, we applied spectral normalization to all convolutional layers within the discriminator network, by doing so, the discriminator's learning becomes more stable and the GAN training process converges more reliably [43], whereas, an attention mechanism that is integrated into the generator to help the network focus on anatomically relevant regions, enhancing detail preservation in critical areas of medical images. Figure 2 showing the training pipeline begins by loading image batches, followed by generating enhanced images and calculating both **L1 loss** and **VGG perceptual loss**, which are then combined. Backpropagation is performed, and the model parameters are updated using the **Adam optimizer**, which was configured with custom hyperparameters *(learning rate = 0.0003, $\beta_1 = 0.7$, $\beta_2 = 0.999$)* to improve convergence stability and training efficiency. The process iterates through multiple epochs, with early stopping applied to prevent overfitting. Once optimal performance is reached, the best-performing model is saved automatically. This setup enables the generator to learn how to enhance image quality while preserving structural integrity and minimizing artifacts or distortions.

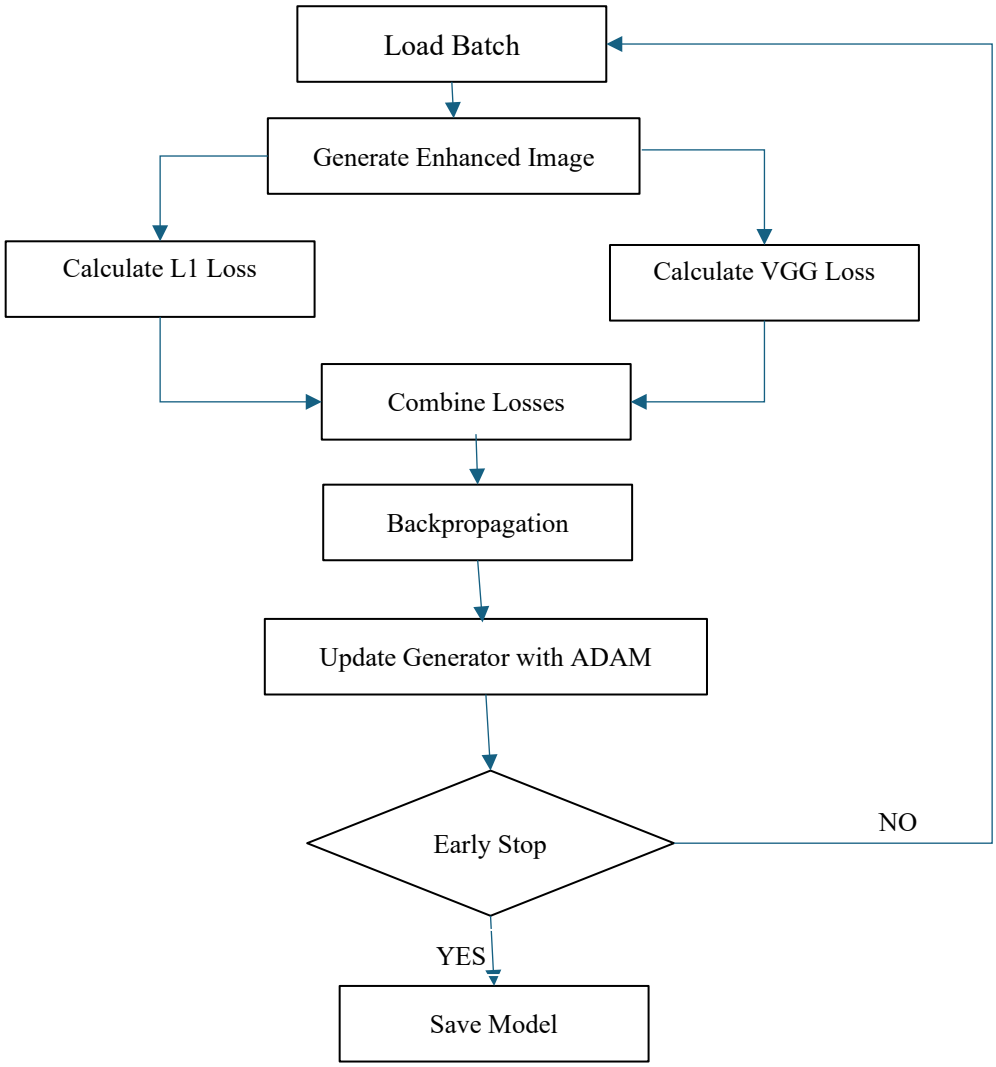

Figure 3. Overview of the Deep Learning Training Workflow Using GAN-Based Generator.

Optimizer Configuration in Deep Learning: Adam with Custom Hyperparameters

The model was trained using the Adam (Adaptive Moment Estimation) optimization algorithm, and adopted early stopping to prevent overfitting. Adam was configured with a learning rate (lr) of 0.0003 and momentum parameters (β_1 and β_2) set to 0.7 and 0.999, respectively. The learning rate of 0.0003 is intentionally kept small to ensure gradual and stable weight updates, minimizing the risk of divergence during training. The first momentum term (β_1=0.7) controls the exponential decay rate for the gradient mean, effectively reducing the influence of past gradients to prevent overshooting local minima. Meanwhile, the second momentum term (β_2=0.999) governs the decay rate for the squared gradients, allowing the optimizer to scale learning rates for each parameter adaptively. This high value ensures robust handling of sparse or noisy gradients, which is particularly beneficial in tasks requiring fine-grained adjustments.

4.3. Evaluation and Saving Phase: Once training is complete, the model's performance is rigorously evaluated using standard objective metrics, including Structural Similarity Index (SSIM), Peak Signal-to-Noise Ratio (PSNR), and Learned Perceptual Image Patch Similarity (LPIPS). These metrics quantitatively assess the visual and structural fidelity of the enhanced images compared to the original inputs. In addition to numerical evaluation, visual comparisons are saved for qualitative analysis. Each stage of the image enhancement process is also archived, offering a complete visual record of the transformation pipeline for transparency and reproducibility.

This research is based on the publicly available "Iris Database" by M. Dobeš and L. Machala (2002) [44], which was obtained from an online source and consists of 384 iris images taken from 64 individuals. Three images were taken of the right eye and three of the left eye of each individual at different times to provide a variety of lighting and image capture conditions. The original images are in color, high resolution, and in JPEG

format. They were converted to grayscale and resized to 256 x 256 pixels before being fed into the optimization model. Figure 3 represents a raw sample of the human iris, serving as the initial input in the proposed image enhancement pipeline. It reflects the typical quality and structural detail encountered in medical imaging before preprocessing. It shows the normal distribution of texture within the iris, making it suitable for training and testing the effectiveness of the optimization algorithms studied. These images were employed in this study to develop and evaluate advanced image enhancement algorithms aimed at improving the quality and diagnostic value of ophthalmic medical photos.

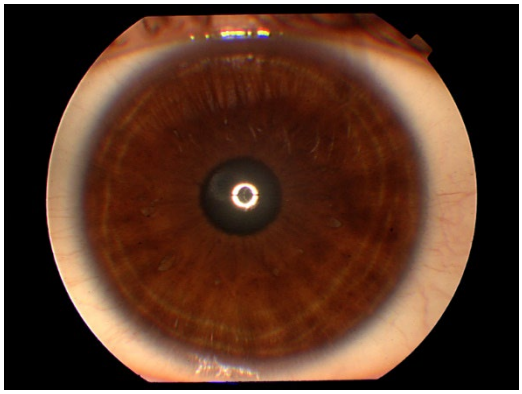

Figure 4. High-Resolution Image of the Human Iris Used as Input for Preprocessing and Enhancement.

5. Result and discussion:

In this work, a series of preprocessing steps was implemented to improve the quality of iris images before entering them into the generative model. As shown in Figure 1, we began by initializing the system setup and preparing the data through the pre-processing phase.

5.1. Pre-processing phase: During this phase, the images underwent a calculated sequence of operations aimed at improving the image's visual properties in terms of contrast, reducing noise, and enhancing details. As shown in Figure 4 This sequence of preprocessing steps, illustrated with a single image, shows how each stage contributes to progressively improving image quality, starting with visual preparation and leading to the sharper image that is later used within the generative model.

The original image, as shown in Figure 4 (A) was first converted to grayscale to ensure processing consistency and facilitate handling of image properties in the deep learning phases, aiming to simplify the visual representation and focus on the textural details within the iris, as shown in Figure 4 (B) Next, the CLAHE algorithm was applied to improve local contrast, which helped highlight fine features in areas that were low in comparison in the original image. This effect is shown in Figure 4 (C).

This was followed by applying a Bilateral filter to remove noise while preserving edge detail. This smoothed the image, as shown in Figure 4 (D). In the final processing step, the Unsharp Masking technique was used to enhance sharpness in fine edges and increase the clarity of details, producing a visually more transparent image that is more ready for analysis, as shown in Figure 4 (E).

It is important to note that the name "Unsharp Masking" can be misunderstood as referring to reducing sharpness. In reality, this method is used to highlight edges and clarify the image. This name comes from traditional photographic techniques, where an unsharp mask was used to enhance the localized edge contrast of the original image [45]. Therefore, despite the name, the final output is a sharpened image, which justifies its software designation in this work.

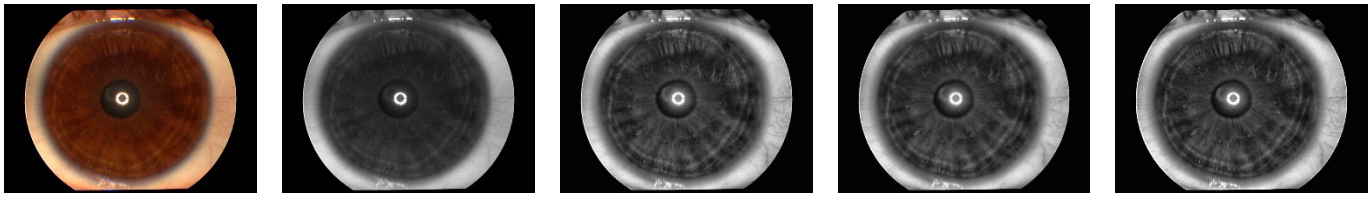

A	B	C	D	E
Original Image	Gray image The original image after converting to grayscale.	CLHE The result of contrast enhancement using the CLAHE algorithm.	Denoised (Bilateral Filter) The result of noise removal using the Bilateral filter.	Sharpened (Unsharp Masking) The result of edge sharpening using the Unsharp Masking technique.

Figure 5. Sequence of preprocessing steps for a single image from the iris database.

The processed image is then fed into the training phase, as shown in the Figure 1.

5.2. Model and training phase: After completing the preprocessing phase, we moved to the generative enhancement phase using a Generative Adversarial Network (GAN)-based framework. As illustrated in Figure 2, the training design

combines pixel-level (L1) and perceptual (VGG) losses, helping the generator produce outputs that are both structurally accurate and visually consistent. The integration of the Adam optimizer and early stopping mechanism proved effective in stabilizing training and avoiding overfitting. These strategies contributed directly to the high-quality enhancement results, as observed in the visual outputs and supported by the obtained evaluation metrics.

An enhanced generator was designed with attention blocks to support the medical image enhancement process by enhancing fine details while preserving the original visual structure. This generator was trained using the Adam initialization algorithm, with hyperparameters (lr = 0.0003, β_1 = 0.7, β_2 = 0.999), which accelerated convergence and reduced loss value. This initialization helped achieve adequate training stability, which positively impacted the quality of the resulting images and supports the efficiency of the framework proposed in this research.

Compared to the default Adam settings (typically lr=0.001, β_1=0.9, β_2=0.999), this configuration prioritizes cautious updates over aggressive convergence, making it well-suited for complex, non-convex optimization landscapes. The reduced β_1 value (0.5 instead of 0.9) further mitigates oscillations, while retaining the adaptive benefits of β_2 near its default. Empirical evidence suggests that such hyperparameters enhance training stability in GANs and other architectures sensitive to hyperparameter tuning. However, they may require longer training times due to the conservative learning rate. This Adam variant strikes a balance between momentum-driven acceleration and adaptive gradient scaling, making it a pragmatic choice for generative and high-precision discriminative tasks. Data augmentation techniques, such as random rotations and horizontal flips, were also applied.

Figure 5 provides a visual comparison between the original grayscale iris image (left) and the output produced by the proposed enhancement framework (right). As is evident, the enhanced image displays improved structural clarity and finer texture details, particularly in the central and peripheral regions of the iris. This qualitative improvement aligns with the quantitative results obtained using standard evaluation metrics, where the enhanced images achieved an average SSIM of 0.9783, LPIPS of 0.00776, and PSNR of 32.22 dB. These metrics confirm that the enhancement process preserved perceptual and structural features while reducing noise and improving contrast—critical factors for subsequent diagnostic or biometric tasks.

5.3. Evaluation and Saving Phase: the enhanced images were evaluated quantitatively using SSIM, LPIPS, and PSNR metrics to assess both structural fidelity and perceptual quality comprehensively.

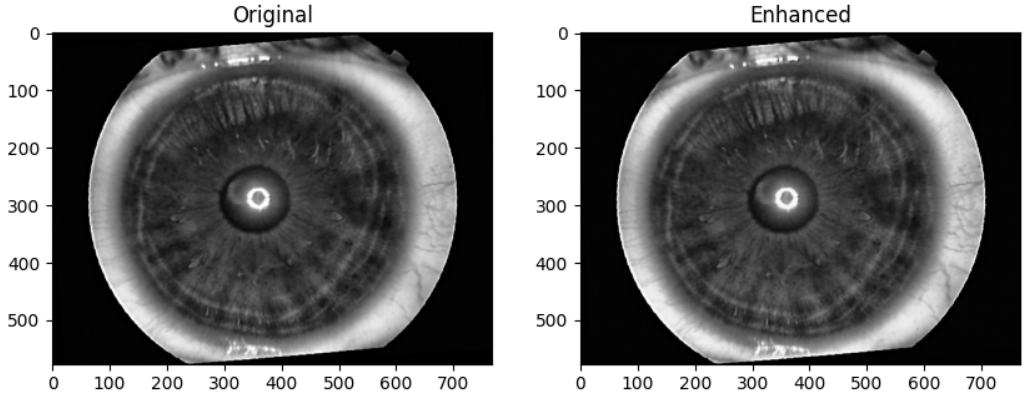

Figure 6. Original vs. enhanced Iris image.

According to the obtained metric values, the framework using tuned hyperparameters outperformed the default configuration across all three key image quality metrics—SSIM, LPIPS, and PSNR—as detailed in Table 1. The average SSIM improved from 0.938347 (default) to 0.978272 (tuned). At the same time, the LPIPS score decreased from 0.013732 to 0.007760, and the PSNR increased from 28.6244 dB to 32.2296 dB, indicating superior structural fidelity, perceptual similarity, and noise resilience, respectively. Furthermore, the standard deviation values reveal an essential aspect of consistency in the output quality. The STD for SSIM decreased from 0.044672 to 0.015213, indicating more stable structural similarity across enhanced images, which is essential for maintaining diagnostic reliability. Similarly, LPIPS showed a reduction in STD from 0.004752 to 0.002139, suggesting reduced fluctuation in perceptual quality. For PSNR, the STD decreased from 3.587311 to 2.429014, reinforcing the consistency in noise suppression and image clarity. These findings confirm that the tuned configuration not only improves average performance but also ensures reliable, repeatable enhancement quality—an essential requirement for medical imaging applications.

To compare the overall values (SSIM, LPIPS, and PSNR) of the dataset images, Figure 6 shows the Dominance in mostly results of hyper-parameter over default parameter, where the values for SSIM are close to 1, values of LPIPS are achieved at

higher values, and PSNR are close to zero, more than the default parameter.

Table (1): Quantitative Evaluation Results: Standard Deviation and Average of SSIM, LPIPS, and PSNR for Enhanced Medical Images Using Tuned vs. Default Parameters.

	Hyper parameter			**Default parameter**		
	SSIM	LPIPS	PSNR	SSIM	LPIPS	PSNR
STD	0.015213	0.002139	2.429014	0.044672	0.004752	3.587311
AVERAGE	0.978272	0.00776	32.22958	0.938347	0.013732	28.6244

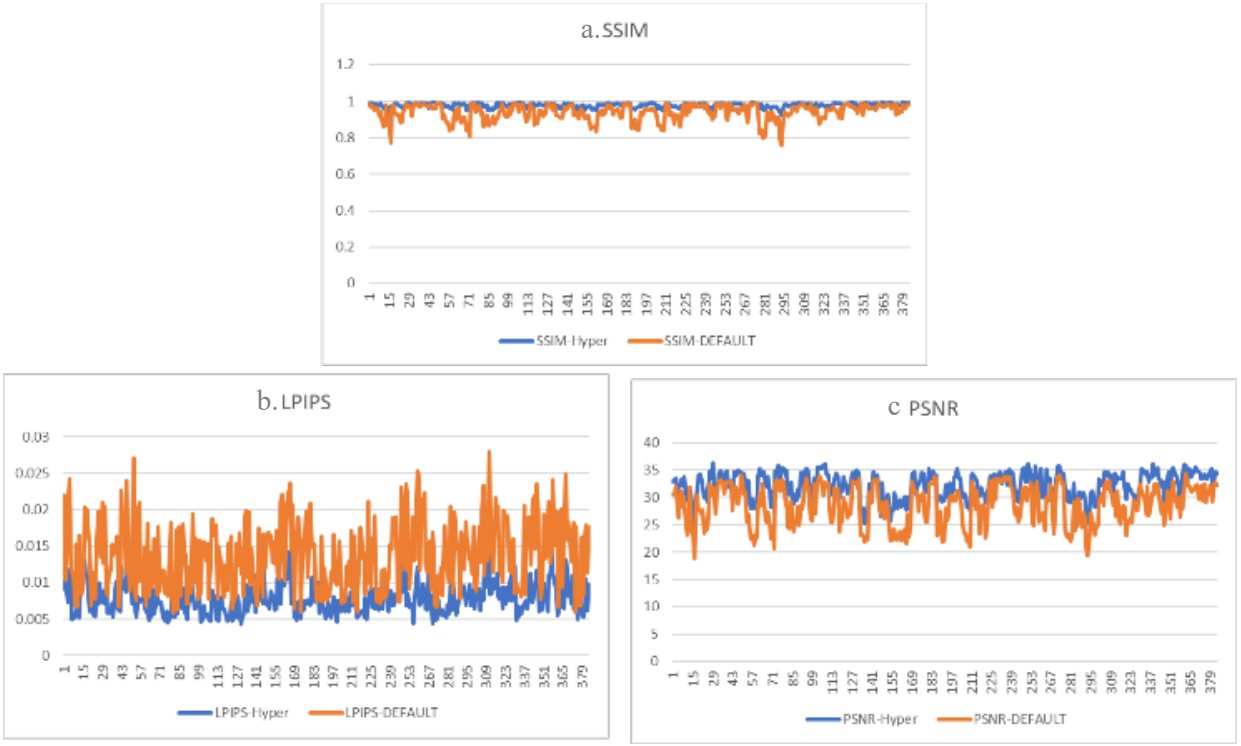

Figure 7. Quantitative comparison of three image quality metrics between default and optimized hyperparameter configurations in medical image enhancement. (a) Structural Similarity Index (SSIM): Evaluates how well the enhanced image preserves the structural information of the original. (b) Learned Perceptual Image Patch Similarity (LPIPS): Measures perceptual differences between original and enhanced images; lower values indicate better visual quality. (c) Peak Signal-to-Noise Ratio (PSNR): Estimates the clarity of the image after enhancement; higher values suggest reduced noise and better quality.

Comparing the results obtained in this research with those of previous studies, it is clear that the proposed model has achieved advanced performance. For example, the average SSIM in this work was 0.978, compared to 0.848 in Mahboubisarighieh et al.'s [15]and 0.8423 in Abdusalomov et al.'s [16], reflecting the current model's ability to recover the image texture to a higher degree. The PSNR also showed a significant increase to 32.22 dB, exceeding the values recorded in the two previous studies (25.46 and 28.45 dB, respectively), indicating a further reduction in information loss. Furthermore, the LPIPS value in the current model was 0.00776, which is significantly lower than the value of 0.152 recorded in Mahboubisarighieh et al.'s study, demonstrating a significant improvement in the quality of visual perception. These comparisons indicate that the proposed model excels in terms of optical and structural efficiency, enhancing its potential for practical use in precision medicine applications.

Conclusion

This study presented an advanced GAN-based framework for medical image enhancement, focusing on improving diagnostic image quality through a carefully designed preprocessing pipeline and customized training strategy. The systematic processing sequence has contributed to improving the quality of medical images used, enhancing the accuracy of disease diagnosis based on image analysis.

The results demonstrated that hyperparameter tuning significantly improved performance across key evaluation metrics—achieving an average SSIM of **0.9783**, LPIPS of **0.00776**, and PSNR of **32.22 dB**—compared to default settings and other state-of-the-art methods. Furthermore, the reduced standard deviations (SSIM STD = **0.0152**, LPIPS STD = **0.0021**, PSNR STD = **2.4290**) reflect enhanced consistency and robustness in output quality. These findings highlight the importance of proper hyperparameter optimization and targeted loss functions in achieving reliable, high-fidelity medical image enhancement suitable for clinical applications.

Future research may focus on enhancing the capabilities of deep learning methods to achieve comprehensive coverage that can be generalized to all medical images, and artificial intelligence networks can be incorporated into the preprocessing stage.

Acknowledgement

The author would like to express they're thanks to the College of Computer Sciences and Mathematics, University of Mosul, for their support of this paper.

Conflict of interest

None.

References

[1] A. Suman, P. Suman, S. Padhy, N. Kumar and A. Sing, "Healthcare revolution: Advances in AI-driven medical imaging and diagnosis," Responsible and Explainable Artificial Intelligence in Healthcare, pp. 155-182, 2025. https://doi.org/10.1016/B978-0-443-24788-0.00007-8

[2] A. Haleem, M. Javaid, R. P. Singh and R. Suman, "Medical 4.0 technologies for healthcare: Features, capabilities, and applications," Internet of Things and Cyber-Physical Systems, vol. 2, pp. 12-30, 2022. https://doi.org/10.1016/j.iotcps.2022.04.001 .

[3] K. J. Zuiderveld, "Contrast limited adaptive histogram equalization," Graphics gems, vol. 4, no. 1, pp. 474-485, 1994. https://doi.org/10.1016/b978-0-12-336156-1.50061-6 .

[4] A. N. Younis and F. M. Ramo, "Detecting Skin Cancer Disease Using Multi Intelligent Techniques," International Journal of Mathematics and Computer Science, vol. 16, no. 4, pp. 1783-1789, 2021.

[5] Y. Ma, J. Liu, Y. Liu, H. Fu, Y. Hu, J. Cheng and Y. Zhao, "Structure and illumination constrained GAN for medical image enhancement," IEEE Transactions on Medical Imaging, vol. 40, no. 12, pp. 3955-3967, 2021. https://doi.org/10.1109/tmi.2021.3101937

[6] F. Spagnolo, P. Corsonello, F. Frustaci and S. Perri, "Design of approximate bilateral filters for image denoising on FPGAs," IEEE Access, 2023. https://doi.org/10.1109/access.2022.3233921

[7] M. K. K. Masood, E. N. Baro and P. O. Roth, " A Novel Intensity-Corrected Blue Channel Compensation and Edge-Preserving Contrast Enhancement Using Laplace Filter and Sigmoid Function for Sand-Dust Image Enhancement," IEEE Access, 2025. https://doi.org/10.1109/access.2025.3548972

[8] Z. Zhang, A. J. Yezzi and G. Gallego, "Formulating event-based image reconstruction as a linear inverse problem with deep regularization using optical flow," IEEE Transactions on Pattern Analysis and Machine Intelligence, vol. 45, no. 7, pp. 8372-8389, 2022. https://doi.org/10.1109/tpami.2022.3230727

[9] N. Seliya, A. A. Zadeh and T. M. Khoshgoftaar, "A literature review on one-class classification and its potential applications in big data," Journal of Big Data,2021. https://doi.org/10.1186/s40537-021-00514-x

[10] A. N. Bishop and P. Del Moral, "On the mathematical theory of ensemble (linear-Gaussian) Kalman–Bucy filtering," Mathematics of Control, vol. 35, no. 4, pp. 835-903, 2023. https://doi.org/10.1007/s00498-023-00357-2

[11] S. Sharif, R. A. Naqv, M. Biswa and W.-K. Loh, "Deep Perceptual Enhancement for Medical Image Analysis," IEEE Journal of Biomedical and Health Informatics, vol. 26, no. 10, pp. 4826-4836, 2022. https://doi.org/10.1109/jbhi.2022.3168604

[12] K. G. Dhal, A. Das, S. Ray, J. Gálvez and S. Das, "Histogram equalization variants as optimization problems: a review," Archives of Computational Methods in Engineering, vol. 28, pp. 1471-1496, 2021. https://doi.org/10.1007/s11831-020-09425-1

[13] I. S. Mohammed and M. K. Hussien, "Off-line handwritten signature recognition based on genetic algorithm and Euclidean distance," IAES International Journal of Artificial Intelligence, vol. 12, no. 3, p. 1238~1249, 2023. https://doi.org/10.11591/ijai.v12.i3.pp1238-1249

[14] V. Sampath, I. Maurtua, J. J. A. Martin and A. Gutierrez, "A survey on generative adversarial networks for imbalance problems in computer vision tasks," Journal of Big Data vol. 8, no. 27, 2021. https://doi.org/10.1186/s40537-021-00414-0

[15] A. Mahboubisarighieh, H. Shahverdi, S. J. Nesheli, M. A. Kermani, M. Niknam, M. Torkashvand and S. M. Rezaeijo, "Assessing the efficacy of 3D Dual-CycleGAN model for multi-contrast MRI synthesis," Egyptian Journal of Radiology, vol. 55, no 118, 2024. https://doi.org/10.1186/s43055-024-01287-y

[16] A. Abdusalomov, S. Mirzakhalilov, Z. Dilnoza, K. Zohirov, R. Nasimov, S. Umirzakova and Y. Cho, "Lightweight Super-Resolution Techniques in Medical Imaging: Bridging Quality

and Computational Efficiency," Bioengineering (Basel), vol. 11, no. 12, 2024.
https://doi.org/10.3390/bioengineering11121179

[17] P. Pawar, B. Ainapure, M. Rashid, N. Ahmad, A. Alotaibi and S. S. Alshamrani, "Deep learning approach for the detection of noise type in ancient images," Sustainability, vol. 14, no. 18, p. 11786, 2022.
https://doi.org/10.3390/su141811786

[18] M. Momeny, A. M. Latif, M. A. Sarram, R. Sheikhpour and Y. D. Zhang, "A noise robust convolutional neural network for image classification," Results in Engineering, vol. 10, p. 100225, 2021.
https://doi.org/10.1016/j.rineng.2021.100225

[19] V. D. P. Jasti, A. S. Zamani, K. Arumugam, M. Naved, H. Pallathadka and F. Sammy, "Computational technique based on machine learning and image processing for medical image analysis of breast cancer diagnosis," Security and communication networks, vol. 2022, no. 1, p. 1918379, 2022.
https://doi.org/10.1155/2022/1918379

[20] S. Guo, M. Li, Y. Li, J. Chen, H. K. Zhang, L. Sun, Wang J., Wang R. and Y. Yang, "The improved U-STFM: a deep learning-based nonlinear spatial-temporal fusion model for land surface temperature downscaling," Remote Sensing, vol. 16, no. 2, p. 322, 2024.
https://doi.org/10.3390/rs16020322

[21] R. Sepasdar, A. Karpatne and M. Shakiba, "A data-driven approach to full-field nonlinear stress distribution and failure pattern prediction in composites using deep learning," Computer Methods in Applied Mechanics and Engineering, vol. 397, p. 115126, 2022.
https://doi.org/10.1016/j.cma.2022.115126

[22] Z. Chen, K. Pawar, M. Ekanayake, C. Pain, S. Zhong and G. F. Egan, "Deep learning for image enhancement and correction in magnetic resonance imaging—state-of-the-art and challenges," Journal of Digital Imaging, vol. 36, pp. 204-230, 2 2023.
https://doi.org/10.1007/s10278-022-00721-9

[23] I. M. Mohammed and N. A. M. Isa, "Contrast Limited Adaptive Local Histogram Equalization Method for Poor Contrast Image Enhancement," IEEE Access, vol. 13, pp. 62600 - 62632, 2025.
https://doi.org/10.1109/access.2025.3558506

[24] A. Fawzi, A. Achuthan and B. Belaton, "Adaptive clip limit tile size histogram equalization for non-homogenized intensity images," IEEE Access vol. 9, pp. 164466 - 164492, 2021.
https://doi.org/10.1109/access.2021.3134170

[25] J. Liu, X. Zhou, Z. Wan, X. Yang, W. He, R. He and Y. Lin, "Multi-scale FPGA-based infrared image enhancement by using RGF and CLAHE," Sensors, vol. 23, no. 19, 2023.
https://doi.org/10.3390/s23198101

[26] M. M. Khattab, A. M. Zeki, A. A. Alwan, B. Bouallegue, S. S. Matter and A. M. Ahmed, "Regularized Multiframe Super-Resolution Image Reconstruction using Linear and Nonlinear Filters," Journal of Electrical and Computer Engineering, vol. 2021, no. 1, p. 8309910, 2021.
https://doi.org/10.1155/2021/8309910

[27] P. Lu and Q. Huang, "Robotic weld image enhancement based on improved bilateral filtering and clahe algorithm," Electronics, vol. 11, no. 21, 2022.
https://doi.org/10.3390/electronics11213629

[28] H. Li and X. L. Duan, "SAR ship image speckle noise suppression algorithm based on adaptive bilateral filter," Wireless Communications and Mobile Computing, vol. 2022, no. 1, p. 9392648, 2022.
https://doi.org/10.1155/2022/9392648

[29] J. Mao, Z. Wu and X. Feng, "Image definition evaluations on denoised and sharpened wood grain images," Coatings, vol. 11, no. 8, 2021.
https://doi.org/10.3390/coatings11080976

[30] H. A. Jalab, M. A. Alqarni, R. W. Ibrahim and A. A. Almazroi, "A novel pixel's fractional mean-based image enhancement algorithm for better image splicing detection," Journal of King Saud University-Science, vol. 34, no. 2, p. 101805, 2021.
https://doi.org/10.1016/j.jksus.2021.101805

[31] Y. Wang and J.J. Healy, " Image Quality Assessment for Gibbs Ringing Reduction," Algorithms, vol. 16, no. 2, 2023.
https://doi.org/10.3390/a16020096

[32] X. Yi, E. Walia and P. Babyn, "Generative Adversarial Network in Medical Imaging: A Review," Medical Image Analysis, vol. 58, 2019.
https://doi.org/10.1016/j.media.2019.101552

[33] R. K. Remya, K. R. Vidya and M. Wilscy, "Detection of deepfake images created using generative adversarial networks: A review." Second International Conference on Networks and Advances in Computational Technologies: NetACT 19. Cham: Springer International Publishing, pp. 25-35, 2021.

[34] E. Strelcenia and S. Prakoonwit, "A survey on GAN techniques for data augmentation to address the imbalanced data issues in credit card fraud detection," Machine Learning and Knowledge Extraction, vol. 5, no. 1, 2023.
https://doi.org/10.3390/make5010019

[35] A. Figueira and B. Vaz, "Survey on synthetic data generation, evaluation methods and GANs," Mathematics, vol. 10, no. 15, 2022.
https://doi.org/10.3390/math10152733

[36] M. M. Sanja, Z. Lukac and M. Temerinac. "Objective estimation of subjective image quality assessment using multiparameter prediction," IET Image Processing, vol. 13, no. 13, 2019.
https://doi.org/10.1049/iet-ipr.2018.6143

[37] A.M. Adeshina, S. Abdul Razak, S. Yogarayan and M. S. Sayeed "Measuring Fidelity of Steganography Approach in Securing Clinical Data Sharing Platform using Peak Signal to Noise Ratio (PSNR) and Structural Similarity Index Measure (SSIM)," *Informatica, vol.* 49, no. 11, 2025.
https://doi.org/10.31449/inf.v49i11.5661

[38] V. Mudeng, M. Kim and S. Choe, "Prospects of structural similarity index for medical image analysis," Applied Sciences, 2022.
https://doi.org/10.3390/app12083754

[39] O. Sjögren, G. G. Pihlgren, F. Sandin and M. Liwicki, "Identifying and Mitigating Flaws of Deep Perceptual Similarity Metrics, Proceedings of the Northern Lights Deep Learning Workshop 2023", vol. 4, 2023.
https://doi.org/10.7557/18.6795

[40] S. Czolbe, P. Pegios, O. Krause and A. Feragen, " Semantic similarity metrics for image registration ," Medical Image Analysis, vol.. 87, no. 102830, 2023, https://doi.org/10.1016/j.media.2023.102830

[41] X. Sun, N. Gazagnadou, V. Sharma, L. Lyu, H. Li and L. Zheng " Privacy Assessment on Reconstructed Images: Are Existing Evaluation Metrics Faithful to Human Perception?," 37th Conference on Neural Information Processing Systems (NeurIPS 2023), vol. 36, pp. 10223--10237, 2023.

[42] M. Arabboev, S. Begmatov, M. Rikhsivoev, K. Nosirov and S. Saydiakbarov, "A comprehensive review of image super-resolution metrics: classical and AI-based approaches," *Acta IMEKO*, vol. *13, no. 1, pp.* 1-8, 2024. https://doi.org/10.21014/actaimeko.v13i1.1679

[43] Z. Shu and K. Zhang, "Spectral Normalization for Generative Adversarial Networks for Artistic Image Transformation", International Journal of Digital Multimedia Broadcasting, vol. 1, 2024. https://doi.org/10.1155/2024/6644706

[44] M. Dobeš and L. Machala, "Iris Database," 2002. [Online]. Available: http://phoenix.inf.upol.cz/iris/.

[45] R. C. Gonzalez and R. E. Woods, Digital Image Processing (4th ed.), Pearson, 2018.